



HAL
open science

Multiscale aspects of the response of a temperature field to a pulsed laser or a periodic laser spot: some applications for IR thermography for non destructive evaluation, terahertz tomography, super-resolution, and microscale heat transfer

Jean-Christophe Batsale, Emmanuelle Abisset, Fouzia Achchaq, Abderezak Aouali, Stephane Chevalier, Marie-Marthe Groz, Jeremie Maire, Alain Sommier

► To cite this version:

Jean-Christophe Batsale, Emmanuelle Abisset, Fouzia Achchaq, Abderezak Aouali, Stephane Chevalier, et al.. Multiscale aspects of the response of a temperature field to a pulsed laser or a periodic laser spot: some applications for IR thermography for non destructive evaluation, terahertz tomography, super-resolution, and microscale heat transfer. *Thermosense: Thermal Infrared Applications XLV*, Apr 2023, Orlando, United States. 10.1117/12.2665448 . hal-04268561

HAL Id: hal-04268561

<https://hal.science/hal-04268561>

Submitted on 2 Nov 2023

HAL is a multi-disciplinary open access archive for the deposit and dissemination of scientific research documents, whether they are published or not. The documents may come from teaching and research institutions in France or abroad, or from public or private research centers.

L'archive ouverte pluridisciplinaire **HAL**, est destinée au dépôt et à la diffusion de documents scientifiques de niveau recherche, publiés ou non, émanant des établissements d'enseignement et de recherche français ou étrangers, des laboratoires publics ou privés.

Multiscale aspects of the response of a temperature field to a pulsed laser or a periodic laser spot. Some applications for IR thermography for Non Destructive Evaluation, Terahertz tomography, super-resolution and microscale heat transfer.

JC. Batsale, *^a, E. Abisset. F. Achchaq, A. Aouali, S. Chevalier, MM. Groz, J. Maire, A. Sommier

I2M (Institute of Mechanics and Mechanical Engineering of Bordeaux)
Université de Bordeaux, CNRS, Arts et Métiers Paris tech, Bordeaux INP, 351 AV de la Libération, 33405 TALENCE, France

ABSTRACT

The study of the response of a temperature field (recorded from IR cameras) to a laser spot heating is increasingly used for NDE (Non Destructive Evaluation) applications. The most classical type of application is to use the flying spot in order to detect vertical cracks and/or to measure the in plane thermal diffusivity in relation to the observation plane of opaque materials. But several other ways of applications are presented here related to tomography and also super resolution.

Instead of opaque materials applications, the tomography is using the principles of the flying spot. It consists in an indirect detection on an intermediate layer (the thermoconverter) that can convert a wide range of radiation from the spot.

The objective of super-resolution can also be implemented with flying spot in order to circumvent the low spatial resolution of IR imaging systems. Such methods consider spots whose diameter is small compared to the size of the pixel.

Some applications of our team will be shown with multiscale considerations.

Keywords: Flying spot, multiscale analysis, image processing, optical instruments, terahertz radiation, multispectral radiation, tomography, microscale instrumentation.

1. INTRODUCTION

The study of the response of a temperature field to a laser spot heating is a classical and ancient method (see for example [1,2,3]).

In the case of the response of a thick homogeneous medium, the temperature field (impulsive or periodic) has the advantage to give a signal which is deployed on a temperature logarithmic scale which theoretically can correspond to very large or very small space and time scales (see [4]).

The pulsed spot has the advantage of giving a fast response, well suited for NDE, representative of a wide range of time-frequencies with particularities of separability of the temperature field along the two directions of space x and y . However, despite precautions, this mode of excitation gives a response sensitive to the measurement noise. It is used for quick inspections in the industrial domain (see [5]).

The periodic spot (see [6,7]) has the advantage by studying the amplitude and the phase shift to provide information where the measurement noise can be reduced thanks to the repetition of the signal, but at a given frequency. This type of instrumentation is well suited for small scales where the duration of experiment is short.

These methods are not only useful for the characterization of opaque materials, but also for tomography and multispectral applications in semi-transparent media ([8,9,10]).

Finally, the observation of the temperature field with IR camera is limited by the resolution of the instrument and the diffraction limits of the IR radiation. One way to circumvent this problem is to consider the transient response of a pixel averaging the response to a small sized moving spot [11]. Some applications of our team will be shown in the areas mentioned above such as: NDE, tomography, super resolution.

2. CLASSICAL CONSIDERATIONS ABOUT THE FLYING SPOT

One example of the classical experiment so called “Flying Spot” consist in the system presented on figure 1. It consists in a laser beam collimated through an optical collimator system [4]. A dual-axis scanning galvanometric system enables the control of the spatial displacement of the laser spot. The focus of the laser beam on the surface is performed with a f-theta scan lens. In practice, the angular positions of the galvanometric system are related to a couple of coordinates expressed as voltage (V). The beam is reflected with a dichroic mirror. The measurements of the temperature fields are made on a IR camera.

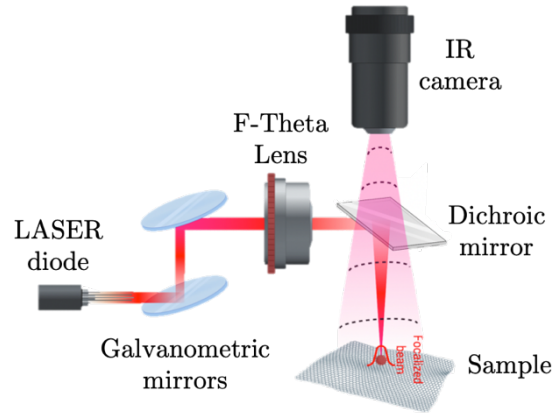


Figure 1: Schematic representation of the flying spot experimental setup.

As a first approximation, the size of the laser spot is considered to be point-like. The heating is either pulsed, time step or periodic. In reality, the laser spot is not purely punctual but the following expressions remain very good approximations in order to understand and explain the signal processing methods [12].

2.1 Analytical temperature response to a pulsed point source

The front face analytical expression of the temperature response field of a pulsed point source, imposed on the front face ($z = 0$) of a homogeneous and anisotropic semi-infinite medium, is written as follows [4]:

$$T(x, y, z = 0, t) = \frac{Q}{\rho c_p} \frac{\exp\left(\frac{(x-x_0)^2}{4a_x t}\right)}{\sqrt{\pi a_x t}} \frac{\exp\left(\frac{(y-y_0)^2}{4a_y t}\right)}{\sqrt{\pi a_y t}} \frac{1}{\sqrt{\pi a_z t}} \quad (1)$$

where x_0, y_0 are the spatial coordinates of the laser spot versus x and y directions (m); a_x, a_y, a_z represent the thermal diffusivities versus the x, y and z directions ($\text{m}^2 \cdot \text{s}^{-1}$); Q is the energy of the pulse point source (J), and ρc_p corresponds to the heat capacity per unit volume ($\text{J} \cdot \text{m}^{-3} \cdot \text{K}^{-1}$). Due to the separability properties, Equation (1) can be divided by the spatial averaged temperature to obtain 2D and transient thermal response.

If the space average following the x and y directions is considered, it yields a 1D transient temperature distribution where the consideration of the spatial logarithm of the previous expression then yields the logarithmic formulation of the temperature vectors. The inverse processing method consists in the estimation of a parabola along x and y directions. The coefficient of order 2 of the fitted parabola allows the estimation of the thermal diffusivity as function of time. Finally, by using a linear fit between this 2 order coefficient and the inverse of the time, a slope corresponding to the thermal diffusivity is obtained. By repeating this operation for each Pulsed Spot a field of in-plane thermal diffusivities along x and y can be retrieved [4].

2.2 Analytical temperature response to a periodic point source

The front face analytical expression of the Fourier transform of the temperature field of a periodic point source, imposed on the front face ($x=x_0, y=y_0, z=0$) of a homogeneous and anisotropic semi-infinite medium, heated by a power P (in W) at pulsation ω , is such as [6]:

$$\bar{T}(x, y, z = 0, \omega) = \frac{P}{2\pi\rho c_p} \frac{\exp\left[-(1+j) \sqrt{\frac{\omega}{z} \left(\frac{(x-x_0)^2}{a_x} + \frac{(y-y_0)^2}{a_y}\right)}\right]}{\sqrt{a_x a_y a_z \left(\frac{(x-x_0)^2}{a_x} + \frac{(y-y_0)^2}{a_y}\right)}} \quad (2)$$

The processing of such signal is considered from the amplitude or the phase of the signal. If the sample is isotropic ($a_x = a_y = a_z$), the logarithm of the amplitude and the phase are linearly depending on the distance from the heating source. It gives a suitable way to estimate the thermal diffusivity. If the sample is non-isotropic the so-called ellipsometry method is suitable in order to estimate the local orientation of fibers in the case of composite materials [7].

The advantage of such method is related to the possibility of repetition of the periodic heating which allow to decrease the influence of the measurement noise. Unlike the previous method, it is not here possible to separate the signal in a product of three simple 1D response.

2.3 Case of multilayered samples

One disadvantage of the previous analytical expressions is that often the medium to be studied is not homogeneous but multilayered or with more complex heterogeneities. Thank to integral transformations of Laplace or Fourier over time and space, it can be shown that the mathematical expressions related to the heat transfer through multilayered media is very similar for pulsed (with Laplace transforms) or periodic cases (with Fourier transform). Asymptotic expansions and analytical approximations are then very useful in order to consider different parts of the signal sensitive to particular groups of parameters (in plane diffusivity, in-depth properties, properties of an equivalent homogeneous medium etc...) [13].

One of the most common cases is to consider a thin coating on a thick sample (assumed to be semi-infinite). The coating layer is approximated as a purely resistive layer or a simple thermal resistance R . By integrating over time, the field averaged in x and y resulting from the expression (1) then gives the response to a step type point heating of intensity q (Wm^{-2}) of the form:

$$\langle T(t) \rangle_{x,y} = \frac{2q}{\sqrt{\lambda_z \rho c_p \sqrt{\pi}}} \sqrt{t} + Rq \quad (3)$$

λ_z is the thermal conductivity following the z direction. The effect of the thermal resistance R is here considered as a shift at the origin ordinate of a 1D behaviour of a purely homogeneous sample.

2.4 Remark about the previous methods

The pulse or periodic approaches need to consider logarithmic scales. They give an evident relation ship between time and space suitable for multiscale analysis. Unfortunately, the application of the previous analytical or even numerical expressions are sensitive to the measurement noise and the instrumentation errors.

If the measurement noise is considered as a random variable e_T so called “Measurement error” and assumed to be additive with constant standard deviation, the measured temperature \hat{T} can be also considered as a random variable related to the real temperature T , such as [14]:

$$\hat{T} = T + e_T \quad (5)$$

The use of the logarithm of the temperature needs then to consider a propagation of the error which is inversely proportionnal to the temperature, such as:

$$\widehat{Ln(T)} = Ln(T) + \frac{e_T}{T} \quad (6)$$

An intuitive way to process these signals is to seek the largest possible signal or the spatial or temporal gradient or temporal variation zones. The signal to noise ratio is then the most favorable.

On the other hand, generally the mean “Measurement error” random variable is assumed to be zero. Then the averaging of the global recording of the frames allows to eliminate the zone where space or temporal gradient are negligible and only to consider the maximum temperatures or maximum gradients.

The success of methods that combine the flying spot with filters that highlight high gradient areas for defect detection come from these considerations [15].

In this spirit we present two examples drawn from the work of our team: the combination of flying spot and thermoconverters (section 3) and super resolution methods (section 4).

3. TERAHERTZ CONSTANT VELOCITY SPOT FOR 3D TOMOGRAPHIC OR MULTISPECTRAL IMAGING

This example reports a terahertz tomography technique using a constant velocity flying spot as a light beam in the terahertz or multispectral domain. In the past, our team developed methods using terahertz radiation consisting of irradiating a large surface and studying the transmission over an entire image [8].

Recently, we have rather tried to concentrate the radiation on a small spot by trying to process the signal at its maximum intensity.

This system consider the light beam capable of partially passing through a semi-transparent medium. A thermoconverter is used as a thin and homogeneous carbon-based film acting as an opaque layer which absorbs the transmitted radiation and transforms it into IR emissions by the calorific effect of photon absorption [9,10].

This thermoconverter is inseted between the IR camera and the object to be tomographed (see figure 2). The transmitted energy is then measured by the simple consideration of the maximum temperature of the image at the passage of the spot. Even of the transmitted energy is weak and even in diffraction limit conditions, the pixel of the maximum temperature is often on the image of the converter the only suitable pixel leaving the measurement noise and comparable with the similar pixel at the next time step. The observation of the spot response on the thermoconverter is an indirect example of flying spot application. All the methods briefly mentioned in section 2 should be revisited to improve and optimize this system.

In this specific case, the source of terahertz radiation is of wavelength equal to $\lambda=3\text{mm}$, held on a translation scanner. It is then suitable for analyzing a semi-transparent object mounted on a rotating stage for the measurement of its absorbance at several angular positions. From the projections made in 2,5 hours and expressed in terms of sinograms, the 2D volume of the absorption coefficient of the object (a vial of hydroalcoholic gel with dimensions equal to $170\text{mm}\times 65\text{mm}\times 50\text{mm}$) is reconstructed by a back-projection method based on the inverse Radon transform.

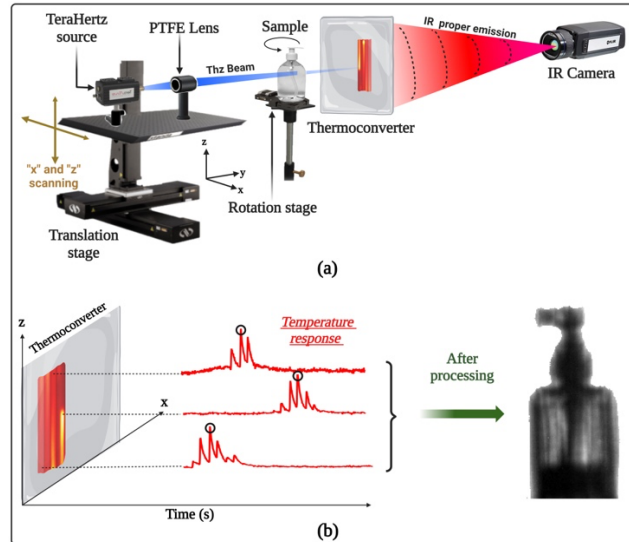


Figure 2: Experimental setup and a priori numerical processing of the acquisitions: **(a)** complete description of the experimental setup dedicated to 3D terahertz imaging; **(b)** Scheme of the numerical processing necessary on each acquired film to obtain a useful image.

This new terahertz volume tomography method thus exhibits the ability to qualitatively reconstruct the volume of physical quantities to the chemical composition of complex shaped and spectrally heterogeneous samples. This approach allows the generation of data cubes that can represent about three million voxels in an averaged time of 2 hours. Therefore, this system opens new perspectives in the field of THz imaging spectroscopy, since the processing of large amounts of data is constantly evolving.

4. ACTIVE THERMAL SUPER RESOLUTION WITH FLYING SPOT

Another application of flying spot is to consider a punctual spot (or here a spot with a small diameter compared to the size of the pixel) moving with constant velocity. If this spot moves on a surface whose limits correspond to the limits targeted by a pixel, then processing of the transient signal will correspond to a super resolution geometrical information.

Even if super resolution methods exist in the domain of classical image processing (see for instance papers related to multiple image based algorithms [17,18]), the investigation of a transient subpixel information given by the heat transfer can be useful in order to increase the physical information quantity. It can then be considered as an “active thermal super-resolution method”.

In order to illustrate this method, a 1D case is proposed by considering 1D sample described on figure 3.

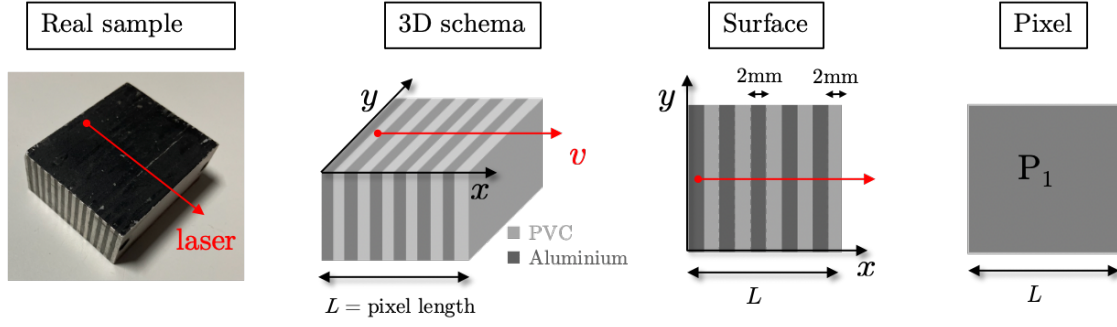


Figure 3: Sample made of multiple layers (PVC, Aluminium). The flying spot will move following the x -direction ($L=20\text{mm}$). The size of the considered pixel is L^2 . In fact, the pixel considered here is the average of a set of pixels targeted by the camera. A black coating is on the front face of the sample.

The flying spot can be used at constant velocity and constant heating or constant velocity with periodic pulses all along the route of the spot. The field of front face ($z=0$) temperature response is considered as averaged versus y -direction and by neglecting the diffusion versus x -direction. It results by integration or super-position of variants of the expression (1).

If the sample is homogeneous and the spot at constant heating and constant velocity: v , the transient signal from the pixel is (for. $0 < t < L/v$):

$$T_{pix}(t) = \frac{2q}{\sqrt{\lambda_z \rho c_p \pi}} \sqrt{t} \quad \text{or} \quad T_{pix}(t) = \frac{2q}{\sqrt{\lambda_z \rho c_p \sqrt{\pi}}} \sqrt{t} + Rq \quad (7)$$

From expression (3), it can be considered that the black painting is acting as a coating layer which influences only the signal by a shift on the origin ordinates. This remark is valid for the following expressions.

For a multilayered sample such as on figure 3, with an index 1 for the first layer and 2 for the second layer.

$H(t)$ is the Heaviside function, with a constant heating q ($W m^{-2}$) it yields (for. $0 < t < L/v$):

$$T(t) = \frac{2q}{\sqrt{\lambda_{z1} \rho c_{p1} \pi}} \sqrt{t} \left(1 - H\left(t - \frac{x_1}{v}\right) \right) + \frac{2q}{\sqrt{\lambda_{z2} \rho c_{p2} \pi}} \sqrt{t} \left(H\left(t - \frac{x_1}{v}\right) - H\left(t - \frac{x_2}{v}\right) \right) + \dots (8)$$

For the same multilayered sample but with pulses of intensity Q ($J m^{-2}$) at time τ_i and τ_k (for. $0 < t < L/v$):

$$T(t) = \sum_i \frac{Q}{\sqrt{\lambda_{z1} \rho c_{p1} \pi \sqrt{t - \tau_i}}} \left(1 - H\left(t - \frac{x_1}{v}\right) \right) + \sum_k \frac{Q}{\sqrt{\lambda_{z1} \rho c_{p1} \pi \sqrt{t - \tau_k}}} \left(H\left(t - \frac{x_1}{v}\right) - H\left(t - \frac{x_2}{v}\right) \right) + \dots (9)$$

4-1 Super resolution with high velocity and constant heating flying spot

Theoretically, the signals given by expression (8) make it possible to delimit zones 1 and 2 by simply identifying the local maxima and minima. However, the influence of measurement noise and the limited number of time steps do not allow a correct estimation. One can see in figures 4 and 5 examples of theoretical and experimental signals obtained at a speed of 2.5 cm/s, with an acquisition frequency of 910 Hz.

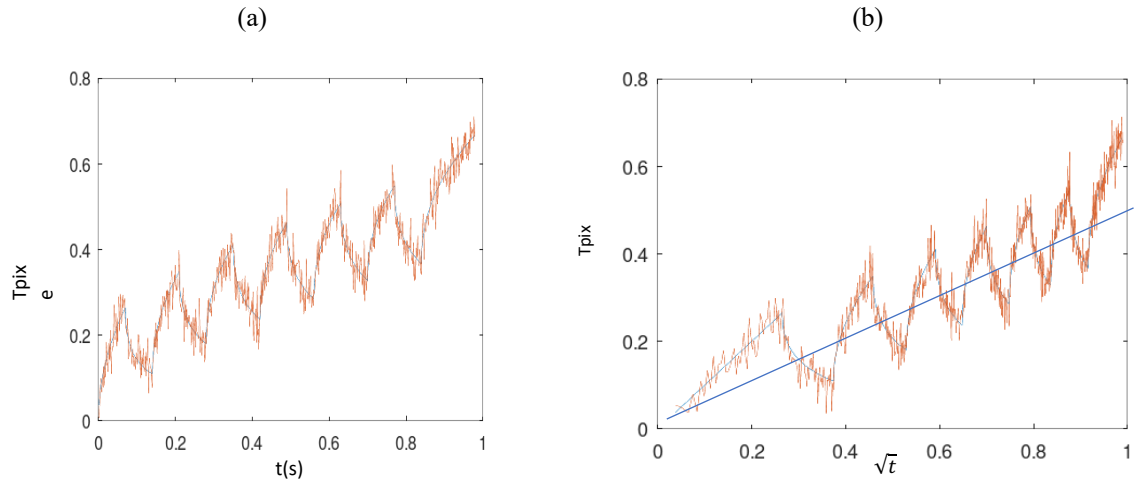


Figure 4: Example of theoretical noisy response of the pixel (a) as a function of time (b) as a function of the square root of time.

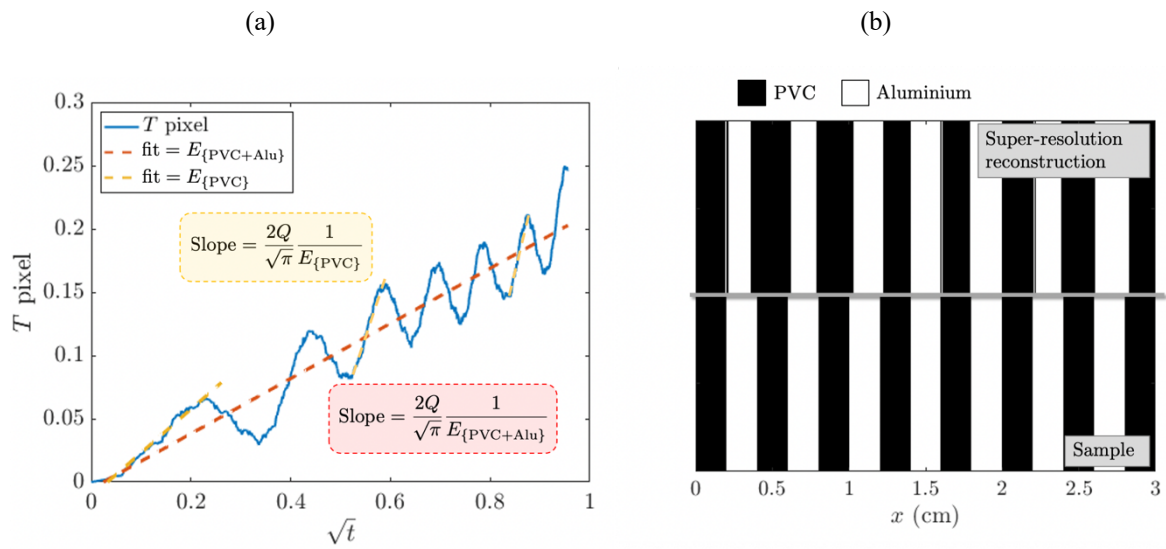


Figure 5: (a) Thermal response obtained for a high laser displacement. (b) Sub-pixel cartography of the sample obtained by the estimation of local maxima and minima.

4-2 Super resolution with low velocity and periodic heating pulses flying spot and wavelet transform analysis

In order to improve the previous results, the low velocity and periodic pulse heating is then implemented. The figure 6 is giving some theoretical examples.

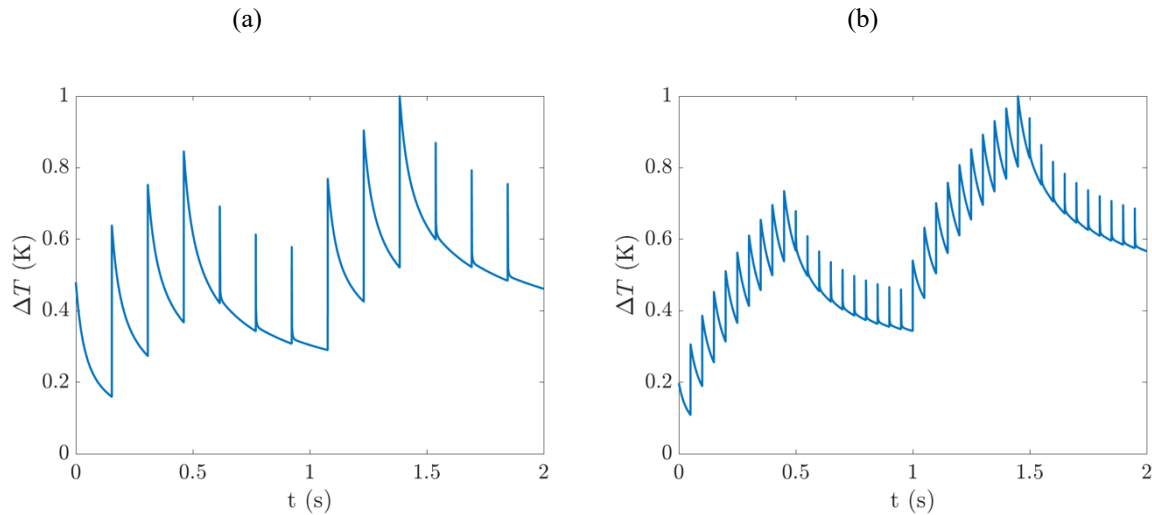


Figure 6 : Results obtained for low laser velocity. Thermograms obtained for (a) 13 laser impacts, (b) 40 laser impacts.

Such signal is more complex than the previous one. The detection of the limits of the heterogeneities is difficult even without additional noise because the local maxima do not necessarily correspond to the interfaces between the layers. However, the signal is richer. It includes both high frequency information and privileged pulse repetition frequencies.

An approach for such signal analysis consists in studying the thermal response with wavelet transform. Wavelet transform is a type of time-frequency analysis that decomposes a signal into a set of wavelets, which are small waves of varying frequencies and durations [19, 20]. They use a family of functions that are both localized in time and frequency. This localization property makes the wavelet transform particularly useful in analyzing signals that have non-stationary features, such as sharp changes in frequency content over time, which is exactly what the super-resolution is looking for. In thermography, wavelet transforms have been used for example to detect and isolate specific features in thermographic images, such as hot spots or thermal anomalies [21,22]. In this paper, the Morlet wavelet transform was chosen for the super-resolution methodology because of its very good ability to capture both high-frequency and low-frequency information.

An illustration of this method is given both to process the numerical case of figure 6 and also to process equivalent experimental cases obtained on the sample presented in figure 3.

On figure 7, each obtained scalogram are a visual representation of the results of the Morlet wavelet transform of the corresponding thermogram. The two-dimensional plot shows the magnitude of the wavelet coefficients as a function of both time and frequency. The x-axis represents time, and the y-axis represents frequency. The magnitude of the wavelet coefficients is indicated by color, with brighter colors indicating larger magnitudes. In this paper, these values are normalized because the focus is made on the localization of the change of thermal properties and not their quantitative values.

The scalogram reveals both the overall structure of the signal and the fine details of its frequency content. By examining the magnitude scalogram, it is possible to identify the dominant frequency components of a signal and how they change over time. In this example, for both experiments, two different patterns can be observed: one in high frequency, the other in low frequency. In order to visualize these results, the focus is then made on the two observed patterns (high frequency and low frequency), marked by dotted lines on the figure 7.a and 7.d, and the results are plotted as function of time for these chosen frequencies.

At high frequency, illustrated on the figure 7.b for the first experiment and 7.e for the second experiment, the information given by the wavelet transform are directly related to the laser impacts. The peak intensities occur at the time of the impact, and the value of the peak are different if the impact is made on the PVC or the Aluminium. As with the first approach, the higher the number of impacts, the more accurate the super-resolution can be. At low frequency, illustrated on the figure 7.c for the first experiment and 7.ef for the second experiment, the information given by the wavelet transform are, in contrast, related to the scale of the material. The high values of intensities occur when the laser is on the PVC and the lowest values are when the impact are on Aluminium. It can be noticed that: the more accurate the super-resolution can be.

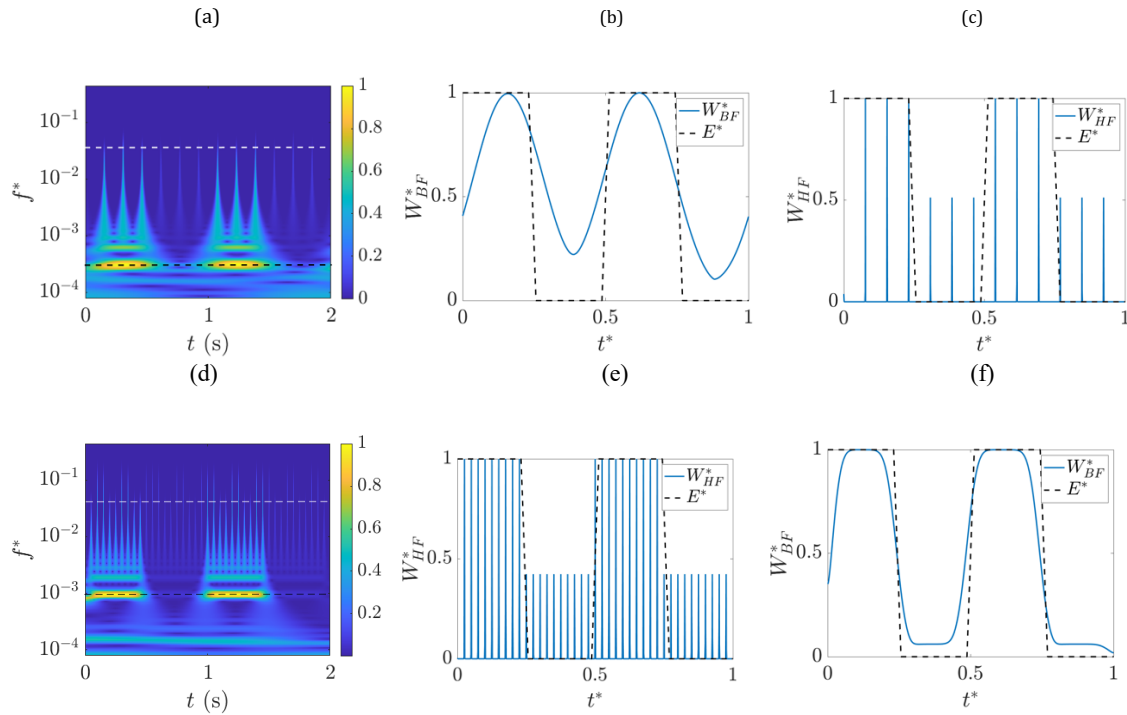


Figure 7: Numerical results obtained for low laser velocity with 13 laser impacts: (a) complete scalogram, (b) focus on high frequency signal and (c) focus on low frequency signal. Numerical results obtained for low laser velocity with 40 laser impacts: (d) complete scalogram, (e) focus on high frequency signal and (f) focus on low frequency signal.

In the case of experimental signal, the studied sample is the same laminate PVC/Aluminium as the one illustrated on figure 3. On a same pixel, three different experiments are performed: 1. $v = 6 \text{ mm.s}^{-1}$ with 50 laser impacts, 2. $v = 2.8 \text{ mm.s}^{-1}$ with 100 laser impacts, 3. $v = 2.3 \text{ mm.s}^{-1}$ with 150 laser impacts.

The laser impacts are uniformly distributed along the x direction for each experiment. The 3 studies are made on the same length of the sample, thus, the distance between two impacts decrease when then number of impacts increases. Therefore, the velocity (and therefore the time) of experimentation is longer for high number of impacts in order to stay in the case of low velocity FS methodology. The obtained thermograms are illustrated on the figure 8:

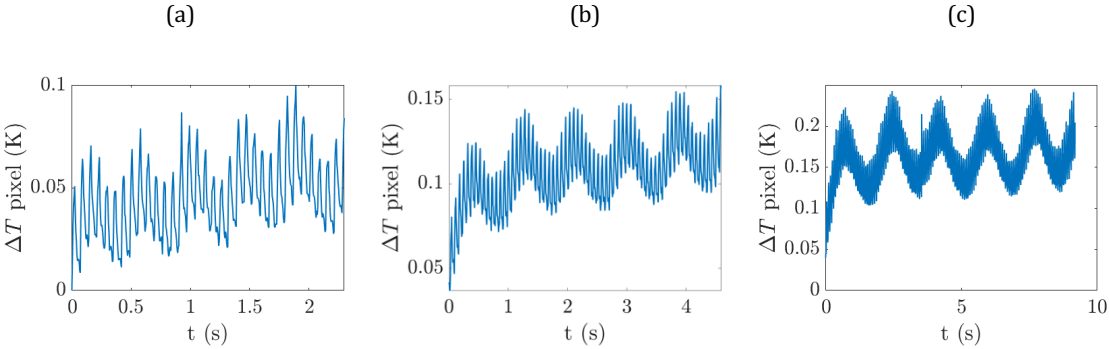
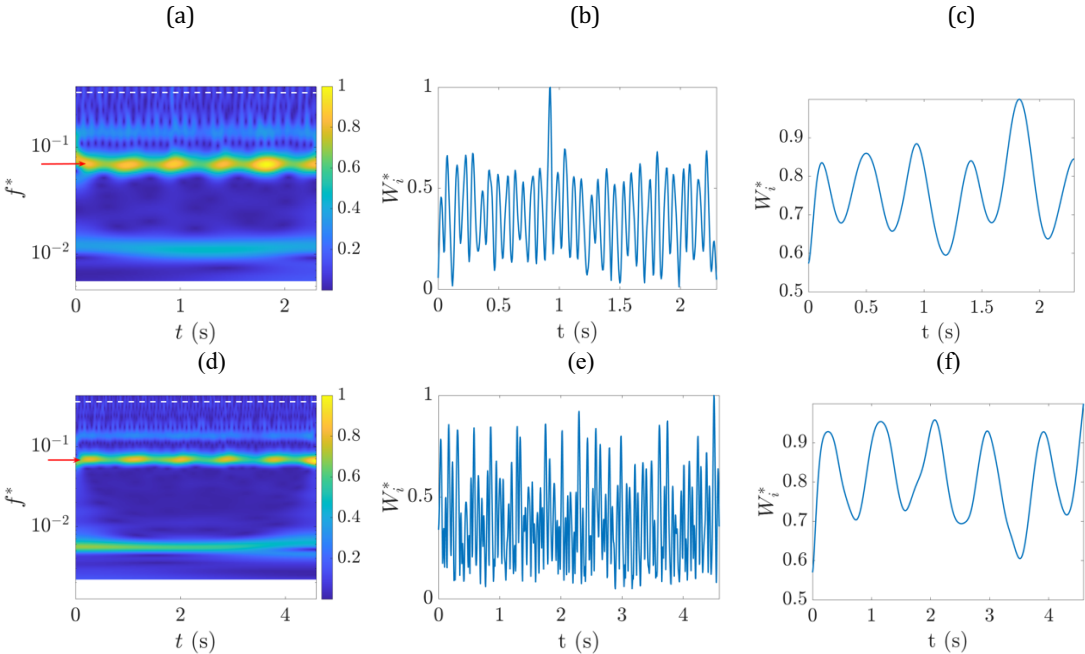


Figure 8: Thermograms obtained for (a) 50 laser impacts, (c) 100 laser impacts and (e) 150 laser impacts on a same pattern of the sample. Sub-pixel cartography obtained with the proposed super-resolution method for (b) 50 laser impacts, (d) 100 laser impacts and (f) 150 laser impacts.

The Morlet wavelet transform are then computed for the three different thermograms and the results are illustrated on figure 9.



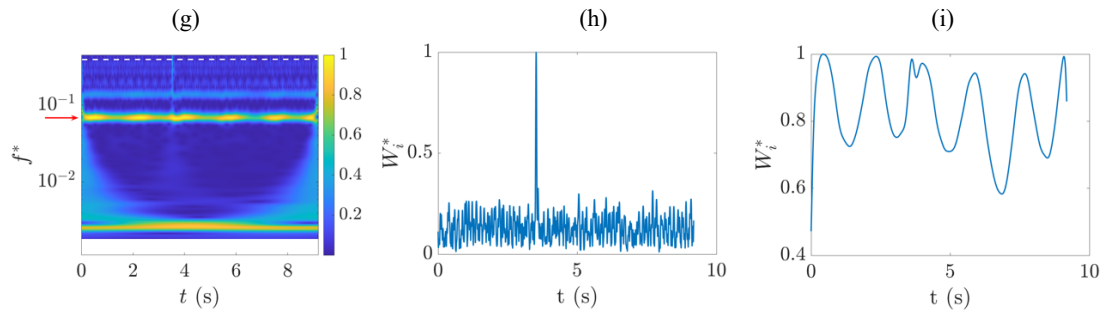


Figure 9: Experimental results obtained for low laser velocity with 50 laser impacts: (a) complete scalogram, (b) focus on high frequency and (c) focus on low frequency. Experimental results obtained for low laser velocity with 100 laser impacts: (d) complete scalogram, (e) focus on high frequency and (f) focus on low frequency. Experimental results obtained for low laser velocity with 150 laser impacts: (g) complete scalogram, (h) focus on high frequency and (i) focus on low frequency.

In the same way as in the previous part, the high frequencies carry information related to the laser impact whereas low frequency carry information related to the scale of the material. The focus is then made on the two observed patterns (high frequency and low frequency), marked by dotted lines and red arrow on the figure 15.a, 15.d and 15.g, and the results are plotted as function of time for these chosen frequencies. Theoretically, it was seen in part 4.2 that at high frequency, high values of intensities occur when the laser is on the PVC and the lowest values occur when impact are on Aluminum.

In this experimental example, these results are difficult to observe because of measurement noise, which is a predominant phenomenon at high frequency. However, at low frequency, measurement noise is not a problem anymore, and the super-resolution methodology is able to perform a sub-pixel cartography: high values of intensities occur when the laser is on the PVC and the lowest values are when the impact are on Aluminum. The limit between the two materials is not perfectly determined but could be by increasing the number of laser impacts.

5. CONCLUSION-PERSPECTIVES

The flying spot method is now a classic method of non-destructive testing and measurement of thermal diffusivity maps. Both pulse and periodic methods can be considered with each having advantages and disadvantages. They must be considered according to the situation encountered (rapid estimation on large scales, precise localized measurements, anisotropy measurements, etc...).

A part from the NDE, new use of these methods can be envisaged in the field of multispectral tomography and also super resolution methods. In the future, the possibilities of piloting the spot associated with techniques of levitation of small samples should allow ever more efficient auscultations. (See a presentation in this same conference on the possibilities offered by acoustic levitation techniques [23]).

By considering intermediary layers (thermoconverters) and a tomographic system it is possible to obtain 3D scans related to the transmittivity of semi-transparent objects. The addition of multispectral sources will open the way for 3D chemical analysis of a large range of transparent solids and fluids.

The perspectives of active thermal super resolution methods presented here are to obtain a higher spatial resolution than the camera. The processing with wavelet transforms are offering a large range of possibilities for multiscale exploration. They constitute an intermediate channel for multiscale processing for signals that are responses to both periodic and pulsed heating.

REFERENCES

- [1] Balageas, D. L. & Busse, G. Theoretical and experimental applications of the flying spot camera. *Proc QIRT 92 Conf. (Seminar Eurotherm No 27)*, Ed. Eur. Therm. Ind. pp. 19–24. (1992). URL www.qirt.org/dynamique/index.php?idD=55. 3
- [2] Krapez, J.-C. Résolution spatiale de la caméra thermique à source volante. *Int. J. Therm. Sci.* 38, 769–779 (1999). 3
- [3] Burrows, S. E., Dixon, S., Pickering, S. G., Li, T. & Almond, D. P. Thermographic detection of surface breaking defects using a scanning laser source. *NDT E Int.* 44, 589–596 (2011). 3
- [4] Gaverina, L., Batsale, J. C., Sommier, A. & Pradere, C. Pulsed flying spot with the logarithmic parabolic method for the estimation of in-plane thermal diffusivity fields on heterogeneous and anisotropic materials. *J. Appl. Phys.* 121 (2017). 3, 5
- [5] Sommier, A. *et al.* Coupling Pulsed Flying Spot technique with robot automation for industrial thermal characterization of complex shape composite materials. *NDT E Int.* 102, 175–179 (2019). URL <https://doi.org/10.1016/j.ndteint.2018.11.011>. 3, 5
- [6] Carslaw HS and Jaeger JC, *Conduction of heat in solids*, 2nd Ed, oxford University Press, 1959
- [7] Krapez JC, Gardette G. Balageas D., Thermal ellipsometry in steady state and by lock in thermography, Application to anisotropic material characterization DOI 10.216011, QIRT, 1996, 042
- [8] Romano, M.; Chulkov, A.; Sommier, A.; Balageas, D.; Vavilov, V.; Batsale, J.; Pradere, C. Broadband Sub-terahertz Camera Based 301 on Photothermal Conversion and IR Thermography. *Journal of infrared, millimeter and terahertz waves* 2016.
- [9] Aouali, A.; Chevalier, S.; Sommier, A.; Abisset-Chavanne, E.; Batsale, J.C.; Pradere, C. 3D infrared thermospectroscopic imaging. *Scientific Reports* **2020**, *10*, 1–10.
- [10] Aouali, A.; Chevalier, S.; Sommier, A.; Ayadi, M.; Batsale, J.C.; Balageas, D.; Pradere, C. Ultra-broadband contactless imaging ²⁹⁹ power meter. *Appl. Opt.* **2021**, *60*, 7995–8005. <https://doi.org/10.1364/AO.432479>.
- [11] Groz MM, Sommier A, ABisset E., Pradere C., Super resolution based on laser Flying Spot technique coupled with OR thermography, QIRT Conference 2022, DOI 10.21611/qirt 2022.3021
- [12] Salazar A., Medioroz A., Oleaga A., Flying spot thermography: Quantitative assessment of thermal diffusivity and crack width, *J. Appl. Phys.*, 127, 131101 (2020) DOI 10.1063/1.5144972
- [13] Maillet D. Andre S., Batsale JC, Degiovanni A., Moyne C., *Thermal quadrupoles*, Wiley, 2000.
- [14] Batsale JC, Pradere C., Time/Sapce noise and thermal processing of temperature signal. EUrotherm Advanced School-Metti 5-Roscoff-June 13-18, 2011. <http://www.sft.asso.fr/document.php?pagendx-12299>
- [15] Schlichting, J., Ziegler, M., Dey, A., Maierhofer, C. & Kreutzbruck, M. Efficient data evaluation for thermographic crack detection. *Quant. Infrared Thermogr. J.* 8, 119–123 (2011). 3

- [16] Guillet JP, Recur B., Frederique L., Bousquet B., Canioni L., Manek-Hnninger I., Desbarats P., Mounaix P., Review of terahertz tomography techniques, *Journal of Infrared Millimeter and Terahertz Waves* 2014, 35 382-411
- [17] Bazzo, J. P. *et al.* Super-resolution algorithm applied in thermal imaging of hydroelectric generators stator using hybrid sensing with DTS and FBG. *SBMO/IEEE MTT-S Int. Microw. Optoelectron. Conf. Proc.* 2015-Decem (2015). 2
- [18] Farsiu, S., Robinson, D., Elad, M. & Milanfar, P. Advances and challenges in super-resolution. *Int. J. Imaging Syst. Technol.* 14, 47–57 (2004). 2
- [19] Yamamoto, A. & T. L. Lee, D. Wavelet Analysis : Theory and Applications. *Hewlett- Packard J.* 44–52 (1994). 9705132v2. 13
- [20] Mourad, T. Wavelets and Wavelet Transforms. *Synth. Lect. Biomed. Eng.* 1–18 (2023). 13
- [21] Galmiche, F. & Maldague, X. Depth defect retrieval using the wavelet pulsed phased thermography 1–6 (2000). 14 , DOI 10.21611/qirt.20222.036
- [22] Shrestha, R., Chung, Y. & Kim, W. Wavelet transform applied to lock-in thermographic data for detection of inclusions in composite structures: Simulation and experimental studies. *Infrared Phys. Technol.* 96, 98–112 (2019). URL <https://doi.org/10.1016/j.infrared.2018.11.008>. 14
- [23] Batsale JC, Achchaq F., Baresh D., Sommier A., Legros P., Strategies for the estimation of thermophysical properties mapping of heterogeneous phase change materials with IR thermography, Thermosence conference, Orlando, May 2023.